Research Square

Preprints are preliminary reports that have not undergone peer review.
They should not be considered conclusive, used to inform clinical practice,
or referenced by the media as validated information.

# Distributed resting-state functional connectivity patterns predict language performance in later adulthood

**Irene Bellin**
University of Padua
**Xueqing Li**
University of Padua
**Arianna Menardi**
University of Padua
**Antonino Vallesi**
antonino.vallesi@unipd.it

University of Padua

**Research Article**

**Keywords:** language performance, predictive modeling, graph theory, reading, comprehension, late adulthood

**Posted Date:** November 4th, 2026

**DOI:** https://doi.org/10.21203/rs.3.rs-10920236/v1

**License:** This work is licensed under a Creative Commons Attribution 4.0 International License. Read Full License

**Additional Declarations:** No competing interests reported.

## Abstract

Language ability in later adulthood depends on functional brain organisation extending beyond classically defined language regions, yet whether resting-state functional connectivity (rs-FC) captures this distributed architecture, and whether predictive information is concentrated within a language-specific network or spread across domain-general systems, remains unclear. Using data from the Human Connectome Project Aging dataset (N = 445; age range: 40–86 years), we combined connectome-based predictive modelling (CPM) and graph-theory analyses to examine the intrinsic neural architecture supporting vocabulary comprehension (TPVT) and single-word reading recognition (READ). CPM yielded significant out-of-sample predictions for both measures (TPVT: r=.233, p=.001; READ: r=.196, p=.001), with predictive edges predominantly spanning inter-network connections across the default mode, fronto-parietal, and dorsal and ventral attention networks; language network edges constituted a non-majority of top-ranked features in both models. Graph-theory analyses of a functionally defined resting-state language network revealed that within-network global efficiency was positively associated with TPVT in lower-educated individuals but negatively so in higher-educated individuals, whose performance was instead linked to greater cross-network connectivity across left temporal, parietal, and prefrontal nodes. Node-wise PCs showed age-dependent reversals in left temporal and temporo-occipital regions for both tasks, with higher cross-network integration benefiting younger but not older adults, consistent with dedifferentiation accounts of cognitive ageing. Together, these findings position language performance in healthy ageing as a whole-brain phenomenon shaped by the interplay between domain-general and language-specific network organisation and its interaction with life-course factors, calling for a shift away from language-centric models toward frameworks that foreground distributed connectivity.

## Introduction

Language is one of the most distinctively human cognitive capacities. Early accounts were shaped by lesion studies implicating discrete cortical regions, most notably Broca's area in speech production and Wernicke's area in comprehension, and by models emphasising the white matter pathways connecting them (Broca, 1865; Geschwind, 1965; Vigneau et al., 2006; Wernicke, 1874). While these classical models offered an influential framework, advances in neuroimaging have since revealed that language cannot be adequately explained solely by damage to, or activity within, any single region. Instead, a growing body of evidence points to language as emerging from a distributed network of interacting cortical regions, subcortical structures, and connecting pathways (Forkel & Hagoort, 2024; Price, 2012; Thiebaut De Schotten et al., 2020), with impairments arising from disruption to broader frontal, temporal, and parietal regions rather than from local regions alone (Dronkers et al., 2004; Price, 2012). Functional neuroimaging has been instrumental in characterising this distributed architecture: language-selective responses concentrate within a left-lateralised frontotemporal network (Lipkin et al., 2022), extending into parietal cortex under increasing linguistic demands (Branco et al., 2020), and this fronto-temporo-parietal organisation appears to generalise across typologically diverse languages, suggesting it reflects fundamental aspects of linguistic cognition rather than the idiosyncrasies of any particular language (Malik-Moraleda et al., 2022).

Despite this evidence, the language network is not consistently recovered as a distinct functional system within commonly used resting-state parcellations. This creates a meaningful methodological gap: task-based approaches reliably identify a language-selective network (Fedorenko et al., 2010; Lipkin et al., 2022), yet this network does not map cleanly onto the canonical large-scale systems extracted from resting-state data at the group level (Fedorenko et al., 2024). This discrepancy likely reflects the field's historical reliance on task-based paradigms to functionally define the core language regions, combined with the fact that spatial averaging across individuals in group-level parcellations can obscure relatively fine-grained or idiosyncratic functional organisation, blurring the boundaries of systems, like the language network, that show substantial inter-individual variability in their precise topography (Braga et al., 2020; Braga & Buckner, 2017; Lipkin et al., 2022).

This does not mean that resting-state data are ill-suited to the study of language. Rather than reflecting language-specific processing, rs-FC captures the intrinsic functional organisation of the brain at rest, a composite of trait-like connectivity patterns, arousal states, physiological fluctuations, and interactions among multiple large-scale systems. In the absence of explicit task demands, rs-FC may offer a task-independent window into the intrinsic organisation of the language network (Braga et al., 2020; Chai et al., 2016; Park et al., 2020). Rs-FC reveals a denser and more complex pattern of inter-regional connections than task-based functional connectivity (Bozzano et al., 2025; Cole et al., 2016; Smith et al., 2009), and captures stable, trait-like individual differences that persist across time (Gratton et al., 2018), making it a theoretically motivated tool for investigating the neural architecture supporting language ability.

A key open question is how broadly the neural basis of language ability is distributed across the brain. Although a specialised language network supports core linguistic processing, domain-general systems are known to interact with it depending on task demands (Hagoort, 2013). Whether individual differences in language ability are primarily reflected in language-network connectivity, or whether predictive information is distributed more widely across large-scale functional systems, remains unclear. Later adulthood provides a theoretically motivated context in which to examine this: ageing is marked by dedifferentiation of large-scale networks and reorganisation of connectivity patterns that may reflect compensatory scaffolding (Stern, 2009; Stumme et al., 2020), while education, a proxy for cognitive reserve, further moderates the connectivity–behaviour relationship (Chan et al., 2014; Stern, 2009).

Two complementary approaches can address these questions at different levels of description. Connectome-based predictive modelling (CPM) uses whole-brain functional connectivity to predict individual differences in behaviour without assuming a priori which regions are relevant, and is well suited to asking both whether rs-FC predicts language ability and where predictive information is concentrated, specifically whether it is confined to a functionally defined language network or extends across domain-general systems (Tomasi & Volkow, 2020). Graph-theory analysis addresses a complementary question: not which connections predict behaviour, but how the topological organisation of a network relates to performance. Prior work has linked such properties to language-related performance (Guichet et al., 2024; Morishima et al., 2025), and reading-related regions appeared distributed across multiple functional networks (Vogel et al., 2013), raising the possibility that the relationship between network topology and language performance may itself be distributed in nature.

The present study addresses these questions using resting-state fMRI and behavioural data from the Human Connectome Project Aging dataset (Harms et al., 2018). Specifically, we asked: (i) Does whole-brain rs-FC predict vocabulary comprehension and word recognition performance in later adulthood, over and above age and education? (ii) Is predictive connectivity concentrated within a functionally defined language network, or distributed across domain-general systems? (iii) Is the topological organisation of the resting-state language network associated with language behavioural performance?

Together, these analyses provide complementary perspectives on the relationship between intrinsic functional organisation and language ability in later adulthood.

## Methods

# Participants

Data were drawn from the Human Connectome Project Aging dataset (HCP-A; Harms et al., 2018). Of the initial 543 participants aged 40 years or older, 98 were excluded because of missing behavioural data or excessive head motion (mean framewise displacement (FD) > 0.5 mm), resulting in a final sample of 445 participants (age range: 40–86 years). Chronological age and years of formal education were extracted as demographic variables and included as covariates in prespecified CPM models and potential moderators of the associations tested in the subsequent analyses.

## Behavioural Measurements: Language Assessments

Language ability was assessed using two NIH Toolbox measures: the Picture Vocabulary Test (TPVT), indexing receptive vocabulary and lexical-semantic comprehension, and the Oral Reading Recognition Test (READ), indexing word-reading recognition and decoding. Age-Corrected Standard Scores (ACSS; Gershon et al., 2014) were used as behavioural outcomes and z-standardised prior to modelling. The same analytical pipeline was applied to NIH Toolbox Flanker Inhibitory Control and Attention scores (Flanker) as a non-language executive-function control measure (see Appendix C). The Flanker analysis was included to establish whether the connectivity–behaviour associations observed for TPVT and READ were specific to language performance or reflected more general relationships between functional network organisation and cognitive ability. Differences in predictive edge profiles and node-wise PC effects between the language measures and Flanker were examined descriptively to assess task specificity.

## fMRI Acquisition and Preprocessing

Neuroimaging data were acquired through the HCP Lifespan protocols (Harms et al., 2018). Structural T1-weighted images were obtained with TR = 2,500 ms, TI = 1,000 ms, and 1 mm isotropic voxel resolution. Resting-state fMRI comprised 488 volumes (TR = 800 ms, TE = 37 ms, voxel size = 2 × 2 × 2 mm, flip angle = 52°).

All data had undergone the HCP Minimal Preprocessing Pipeline prior to access (Glasser et al., 2013), including nonlinear normalisation to MNI space, cortical surface mapping to fsLR32k space, correction for spatial distortion, head motion, and bias field inhomogeneity, and ICA-FIX denoising (Glasser et al., 2016). Following Menardi and colleagues (2024) approach, an additional spatial smoothing was applied using a 6 mm FWHM Gaussian kernel. Data quality control was established by HCP Lifespan procedures (Elam et al., 2021; Marcus et al., 2013).

## Parcellation and the Language Network

We applied a cortical parcellation (400 regions; Schaefer's atlas (Schaefer et al., 2018)) to the preprocessed timeseries, with each parcel assigned to one of seven canonical resting-state networks (Thomas Yeo et al., 2011). To define a functionally grounded language network, we used a validated resting-state language network map (Branco et al., 2020), available on NeuroVault (https://neurovault.org/collections/SARZAHAW/). This map was derived from a seed-based rs-FC analysis with seeds defined from individual

task-fMRI language localiser activations, and reports regions responding selectively to stimuli of increasing linguistic complexity. The group-level t-map was thresholded at high stringency (t > 4), binarised, and overlaid onto the Schaefer's atlas in MNI space. Schaefer's parcels showing a ≥ 51% volumetric overlap with the language mask were reclassified as language network parcels. This procedure yielded 29 language parcels (Fig. 1) spanning predominantly Visual (VIS), Default Mode (DMN), Ventral Attention (VAN), Dorsal Attention (DAN), Sensorimotor (SMN), Frontoparietal (FPN), and Limbic (LIM) regions in the original Yeo nomenclature, producing an 8-network parcellation (the seven Yeo's networks plus a non-overlapping language network; LANG). See Appendix A for a detailed description of parcels' overlap.

## Functional Connectivity

For each participant, a 400 × 400 rs-FC matrix was constructed by computing Pearson correlations between parcel-wise mean BOLD time series, followed by Fisher's z-transformation. The upper triangular elements were retained, yielding 79,800 unique edges per participant. These features served as the input to CPM and as the basis for graph-theoretical analyses.

# Connectome-Based Predictive Modelling (CPM)

An adapted CPM framework was applied as a whole-brain, data-driven framework to test whether rs-FC predicted individual differences in TPVT and READ, without restricting the feature space to the language network a priori (Shen et al., 2017). The distribution of edges related to the predictive model across the 8-network parcellation was then characterised post-hoc. For TPVT and READ, models adjusting for chronological age, years of education, and mean framewise displacement (FD) inside the scanner were designated as the primary model. Three alternative models with different covariates' combinations (mean FD only, age and mean FD, and education and mean FD) were examined as sensitivity analyses and are reported in Appendix B. The fully adjusted model pipeline was also applied to Flanker scores (see Appendix C) as a non-verbal control analysis. Model performance was estimated using a 10-fold cross-validation. Within each training fold, each of the 79,800 edges were correlated with residualised behavioural scores, and those surviving an uncorrected threshold of $p < .01$ were retained as candidate features (Shen et al., 2017). Ridge regression (L2 regularisation) analysis was used to fit the selected edges simultaneously. The regularisation parameter α was optimised via 5-fold inner cross-validation within each outer training fold, selected from 50 log-spaced values ranging from $10^{-2}$ to $10^{5}$. Predictive performance was evaluated using Pearson's r between corresponding covariate-adjusted observed scores and out-of-sample predicted scores, and cross-validated $R^2$ as an error-based accuracy metric. Statistical significance was assessed using 1,000 outcome-label permutation tests, with the permutation p-value calculated as the proportion of permuted correlations ≥ the empirical value (with + 1 correction). For each permutation, outcome labels were randomly reassigned, and the CPM pipeline was repeated using shuffled 10-fold cross-validation, with α fixed to the median value selected across the original-data folds to reduce computational cost. The CPM pipeline was repeated using four additional random seeds, yielding 5 partition schemes and up to 50 valid outer-fold models. These additional repetitions were used for edge-stability analysis and were not averaged into the reported prediction-performance estimates. Edges selected in ≥ 60% of valid folds across the five partition schemes were classified as consensus edges. To rank consensus edges, fold-wise ridge coefficients were L2-normalised and averaged across folds, then weighted by each edge's cross-participant connectivity standard deviation and selection frequency (see Formula a for reference):

1. Ranking score = $|\beta \times SD(edge)| \times$ selection frequency

Elbow detection (*KneeLocator*) was applied to identify a high-ranking subset (top-ranked edges) for network-level characterisation. Edge rankings were treated as descriptive summaries of model-captured information, not as evidence for the independent predictive importance or statistical significance of individual edges. An overview of the adapted CPM workflow is provided in Appendix Figure B1.

## Graph-theory analyses

For each participant, a weighted undirected graph was constructed from the 400 × 400 Fisher-z-transformed FC matrix. To reduce false-positive connections, FDR thresholding (Benjamini–Hochberg, q = .05) was applied to each participant's matrix; non-significant edges and negative correlations were set to zero. Two graph-theory measures capable of quantifying integration patterns were computed using the Brain Connectivity Toolbox in MATLAB (Rubinov & Sporns, 2010). Global efficiency was calculated within the language network subgraph as a measure of within-network integration, reflecting the mean inverse shortest-path length across node pairs. Node-wise Participation Coefficient (PC) was calculated using the full 400-node graph, and then extracted for language network nodes only, indexing the extent to which each node's connections were distributed across functional networks rather than concentrated within the language network. Both metrics were z-standardised prior to Generalized Liner Model (GLM) fitting.

Separate GLMs were fitted for each language measure and each graph-theory metric. For global efficiency, the model included efficiency, age, education, mean FD, and all two-way interactions with efficiency. For node-wise PC, an equivalent model was fitted for each of the 29 language network nodes, with PC, age, education, mean FD, and the corresponding interactions with PC as predictors. Outlying observations were

identified based on initial-fit residuals and excluded before refitting. Node-wise PC models were corrected for multiple comparisons using FDR (Benjamini–Hochberg, q = .05) across the 29 nodes; the global efficiency model required no multiple-comparison correction.

## Results

# Sample Characteristics

Descriptive statistics for age, education and behavioural scores are presented in Table 1. For subsequent modelling analyses, TPVT and READ ACSS were z-standardised separately; however, Table 1 reports the original behaviour ACSS values to retain interpretability.

Table 1
Sample demographic characteristics and behaviour scores

| Variable | Mean | SD | Min | Max |
|---|---|---|---|---|
| **Age (years)** | 63.89 | 11.58 | 40.00 | 85.75 |
| **Education (years)** | 17.53 | 2.14 | 7 | 21 |
| **TPVT ACSS** | 108.75 | 15.11 | 60 | 146 |
| **READ ACSS** | 110.10 | 14.12 | 66 | 146 |

Values are reported for the final sample (*N* = 445). SD = standard deviation; Min = minimum; Max = maximum; TPVT = NIH Toolbox Picture Vocabulary Test; READ = NIH Toolbox Oral Reading Recognition Test; ACSS = age-corrected standard score. TPVT and READ scores are shown in their original ACSS, and z-standardised scores were used in subsequent modelling analyses where specified.

# CPM

The fully adjusted model, in which age, education, and FD were residualised, was treated as the primary CPM model. The remaining covariate-adjustment variants were examined as supplementary sensitivity analyses, and their results are reported Appendix B.

For the TPVT model, the predictive correlation was r = 0.233, permutation *p* = .001, with an error-based cross-validated $R^2$ (CV $R^2$) of 0.005. Among the 124 Top-ranked edges, 30 involved the language network, corresponding to 24.2% of the top-ranked edge set (see Table 2).

For the READ model, the predictive correlation between observed and predicted scores was r = 0.196, permutation p = 0.001, with an error-based CV $R^2$ of − 0.018. Among the 39 Top-ranked edges, 13 involved the language network, corresponding to 33.3% of the top-ranked edge set for the predictive model (see Table 2).

In both tasks, language-related edges represented a non-majority of the Top-ranked edges.

Table 2
**CPM prediction performance and language network attribution for TPVT and READ.**

| Behavioural measure | Covariates residualised | *r* | CV $R^2$ | *Permutation p* | Top-ranked edges, n |
|---|---|---|---|---|---|
| **TPVT** | Age, Education, FD | 0.233 | 0.005 | 0.001 | 124 |
| **READ** | Age, Education, FD | 0.196 | −0.018 | 0.001 | 39 |

Pearson correlation between observed and predicted model-specific scores across held-out folds. Permutation *p* values are based on 1,000 permutations. Top-ranked edges were selected using an elbow-based cutoff applied to the model-based predictive contribution score.

CV $R^2$ = cross-validated coefficient of determination. FD = mean framewise displacement. TPVT = NIH Toolbox Picture Vocabulary Test. READ = NIH Toolbox Oral Reading Recognition Test. Percentages are relative to the total number of Top-ranked edges for each model.

The distribution of top-ranked network pairs in the primary fully adjusted CPM models is presented in Figs. 2 and 3. For TPVT (Fig. 2 - Panel A), 124 Top-ranked edges were identified. The most frequent network pair was the DMN–FPN pair (n = 18, 14.5%), followed by DMN within-network edges (n = 17, 13.7%) and FPN–VAN edges (n = 11, 8.9%). Among LANG-involving edges, the most frequent were DMN–LANG edges and FPN–LANG edges (n = 9 each, 7.3%). For READ, 39 Top-ranked edges were identified as shown in Fig. 2 - Panel B. The most frequent network pairs were the DMN–FPN and DMN–DAN pairs (n = 7 each, 17.9%), followed by FPN–LANG and LANG–VAN edges (n = 5 each, 12.8%). LANG-involving edges accounted for 13 of the 39 Top-ranked edges (33.3%).

DAN = dorsal attention network; DMN = default mode network; FPN = frontoparietal network; LANG = language network; LIM = limbic network; SMN = somatomotor network; VAN = ventral attention network; VIS = visual network.

For both TPVT and READ, Top-ranked edges were predominantly inter-network rather than intra-network edges, accounting for 76.6% and 92.3% of the respective top-ranked edge sets (Fig. 3 - Panel A). For those connections involving LANG nodes, inter-modular connections accounted for the 93.3% and 84.6% of the overall significant edge pairs in predicting TPTV and READ, respectively. Network representation for the endpoints of Top-ranked edges in the primary CPM models is shown in Fig. 3 - Panel B. For TPVT, edge endpoints were most frequently located in the DMN (n = 70, 28.2%), followed by the FPN (n = 49, 19.8%) and the LANG (n = 32, 12.9%). Likewise, edges predictive of READ scores were more likely to have one endpoint in the DMN (n = 21, 26.9%), followed by the FPN (n = 16, 20.5%) and LANG (n = 15, 19.2%).

# General Linear Model Analysis of Language Network Graph Metrics

LANG global efficiency was associated with TPVT and READ performance, after controlling for age, education and mean FD. Interaction terms between global efficiency and each covariate were included to test whether these variables moderated the efficiency–performance association.

For TPVT, the overall model was significant ($F = 11.30$, $p < 0.001$, $R^2 = 0.154$, adjusted $R^2 = 0.140$) (see Table 3). The main effect of language network global efficiency was not significant. However, the Efficiency × education interaction was significant ($\beta = -0.041$, $SE = 0.021$, $t = -1.987$, $p = 0.048$), although close to the conventional .05 threshold. The interaction term indicated a positive association between LANG global efficiency and TPVT at low educational level, but a negative association at high educational level (see Fig. 4).

For READ, the overall model was significant ($F = 10.90$, $p < 0.001$, $R^2 = 0.149$, adjusted $R^2 = 0.135$) *(see Table 4).* No global-efficiency-related terms were statistically significant.

For both TPVT and READ, education was significantly associated with performance (TPTV: $\beta = 0.170$, $SE = 0.020$, $t = 8.429$, $p < 0.001$; READ: $\beta = 0.177$, $SE = 0.021$, $t = 8.612$, $p < 0.001$).

Table 3
LANG global efficiency and TPVT performance.

| Behavioural measure | Model $R^2$ | Adjusted $R^2$ | Model F | model p | Term | β | SE | t | p |
|---|---|---|---|---|---|---|---|---|---|
| TPVT | 0.154 | 0.140 | 11.30 | < .001 | Efficiency | 0.577 | 0.446 | 1.295 | 0.196 |
| | | | | | Age | -0.020 | 0.045 | -0.454 | 0.650 |
| | | | | | **Education** | **0.170** | **0.020** | **8.429** | **< .001** |
| | | | | | FD | 0.289 | 0.501 | 0.575 | 0.565 |
| | | | | | Efficiency × age | 0.027 | 0.044 | 0.606 | 0.545 |
| | | | | | **Efficiency × education** | **-0.041** | **0.021** | **-1.987** | **0.048** |
| | | | | | Efficiency × FD | -0.439 | 0.560 | -0.785 | 0.433 |

Adjusted $R^2$ = adjusted coefficient of determination; FD = mean framewise displacement; LANG = language network; SE = standard error. All main-effect and interaction terms shown were included in the same GLM.

Table 4
**LANG global efficiency and READ performance**.

| Behavioural measure | Model $R^2$ | Adjusted $R^2$ | Model F | model p | Term | β | SE | t | p |
|---|---|---|---|---|---|---|---|---|---|
| READ | 0.149 | 0.135 | 10.90 | < .001 | Efficiency | 0.771 | 0.455 | 1.696 | 0.091 |
| | | | | | Age | -0.015 | 0.046 | -0.337 | 0.736 |
| | | | | | **Education** | 0.177 | 0.021 | 8.612 | **< .001** |
| | | | | | FD | 0.229 | 0.508 | 0.452 | 0.652 |
| | | | | | Efficiency × age | -0.024 | 0.045 | -0.531 | 0.596 |
| | | | | | Efficiency × education | -0.030 | 0.021 | -1.417 | 0.157 |
| | | | | | Efficiency × FD | -0.534 | 0.571 | -0.935 | 0.350 |

Adjusted $R^2$ = adjusted coefficient of determination; FD = mean framewise displacement; LANG = language network; SE = standard error. All main-effect and interaction terms shown were included in the same GLM.

Node-wise linear models were used to test whether node-wise PC in the language network was associated with behavioural performance. The models included PC, age, education, mean FD, and interaction terms between PC and each covariate. Only parcels with significant PC-related terms are reported in Tables 5 and 6.

For TPVT, significant PC-related terms were identified across left temporal, left parietal, left prefrontal, and right temporal regions (see Table 5). The pattern of results was predominantly left-lateralised, with the majority of significant effects involving temporal parcels.

Significant main effects of PC were found in two temporal regions, a left anterior temporal parcel (middle temporal gyrus, anterior portion) and a right posterior temporal parcel (middle temporal gyrus, posterior portion), both showing a negative association between the degree of intermodular edge distribution and TPVT performance. This suggests that greater participation in cross-network communication in these regions is linked to lower receptive vocabulary scores.

The PC × age interactions were also concentrated in the left temporal lobe, involving two adjacent parcels within the posterior superior temporal gyrus, pointing to an age-dependent modulation of hub-like connectivity in this region on TPVT performance. PC × education interactions showed a broader spatial distribution, spanning the left temporal lobe (middle temporal gyrus, posterior portion; superior temporal gyrus, posterior portion), left parietal cortex (supramarginal gyrus/angular gyrus), left prefrontal cortex (inferior frontal gyrus, pars opercularis/triangularis), and the right middle temporal gyrus, the latter being the same region that also showed a significant main effect of PC, suggesting a convergence of PC-related influences on TPVT performance in this right temporal area.

For READ, significant PC-related terms were distributed across left temporo-occipital, left temporal, and right temporal regions (see Table 6). Unlike TPVT, the main effects of PC for READ were positive: greater intermodular connectivity in a left posterior superior temporal gyrus parcel and a right posterior superior temporal gyrus parcel was associated with better reading performance, pointing to a functional role of temporal hub connectivity that is opposite in direction to that observed for receptive vocabulary. The PC × age interactions for READ involved a left temporo-occipital parcel (middle temporal gyrus, temporo-occipital part, extending into the angular gyrus) and a left posterior middle temporal gyrus parcel, both showing negative interactions, a pattern consistent with an age-related attenuation of the connectivity–reading relationship in left temporal association cortex. No significant PC × education interactions were found for READ.

A parcel within the left posterior superior temporal gyrus was the only region yielding a significant PC-related term for both TPVT and READ, yet the nature of the effect differed: for TPVT it emerged as a PC × age interaction, whereas for READ it appeared as a significant main effect of PC. This dissociation suggests that the same region may support vocabulary and reading through partially distinct connectivity mechanisms, with age playing a selective moderating role for receptive vocabulary but not for reading.

The pattern of PC-related findings for TPVT and READ stands in contrast to those obtained for the Flanker task (Appendix C). Although significant PC-related terms were identified for Flanker in overlapping left temporal and left prefrontal parcels (see Table C3), the CPM edge profile for Flanker was dominated by DMN–FPN and within-SMN connections, with language-network parcels accounting for only 27% of the top-ranked edges, a substantially lower proportion than observed for either language measure, and distributed across a different functional architecture. At the node-wise level, the direction of the main effects of PC for Flanker was uniformly negative across all significant parcels, whereas for READ the analogous effects were positive, and for TPVT the pattern was primarily one of age- and education-moderated effects rather than main effects. Notably, the right posterior superior temporal gyrus parcel was the only parcel yielding significant PC-related terms for all three outcomes, yet with opposite directionality for Flanker (negative main effect) relative to READ (positive main effect). Taken together, these contrasts indicate that the PC-related findings for TPVT and READ are not simply a reflection of a non-specific association between cross-network connectivity and general cognitive performance, and that the involvement of left temporal and prefrontal parcels differs qualitatively between language and executive-function tasks.

For education-related interactions, the association was plotted at three representative education levels of 7, 14, and 21 years (Fig. 5). For age-related interactions (Figs. 6 and 7) the association between PC and adjusted behavioural performance was plotted at three representative ages of 40, 63, and 86 years.

Table 5
Significant LANG node-wise participation coefficient (PC) and TPVT performance.

| Behavioural measure | Model $R^2$ | Adjusted $R^2$ | model F | model p | Parcel | Hemisphere / lobe | Significant term | β | SE | t | p |
|---|---|---|---|---|---|---|---|---|---|---|---|
| TPVT | 0.171 | 0.158 | 12.70 | < .001 | 149 | Left middle temporal gyrus | **PC** | -0.847 | 0.421 | -2.012 | **.045** |
| | 0.157 | 0.143 | 11.50 | < .001 | 153 | Left temporal pole | **PC × age** | -0.009 | 0.004 | -2.362 | **.019** |
| | 0.188 | 0.175 | 14.20 | < .001 | 155 | Left middle temporal gyrus | **PC × education** | 0.062 | 0.021 | 2.959 | **.003** |
| | 0.177 | 0.164 | 13.20 | < .001 | 157 | Left superior temporal gyrus | **PC × age** | -0.009 | 0.003 | -2.626 | **.009** |
| | 0.180 | 0.167 | 13.50 | < .001 | 159 | Left supramarginal/angular gyrus | **PC × education** | 0.046 | 0.018 | 2.473 | **.014** |
| | 0.168 | 0.155 | 12.40 | < .001 | 175 | Left frontal gyrus | **PC × education** | 0.055 | 0.020 | 2.734 | **.007** |
| | 0.171 | 0.158 | 12.70 | < .001 | 371 | Right middle temporal gyrus | **PC** | -0.918 | 0.429 | -2.140 | **.033** |
| | 0.171 | 0.158 | 12.70 | < .001 | 371 | Right middle temporal gyrus | **PC × education** | 0.041 | 0.020 | 1.999 | **.046** |

Only significant PC-related terms are shown. Each row reports one significant term from the corresponding parcel-level GLM; consequently, the same parcel may appear more than once. Parcel indices refer to the Schaefer 400-parcel atlas. Adjusted $R^2$ = adjusted coefficient of determination; LANG = language network; PC = participation coefficient; SE = standard error.

Table 6
Significant LANG node-wise participation coefficient (PC) and READ performance.

| Behavioural measure | Model $R^2$ | Adjusted $R^2$ | model F | model p | Parcel | Hemisphere / lobe | Significant term | β | SE | t | p |
|---|---|---|---|---|---|---|---|---|---|---|---|
| READ | 0.154 | 0.141 | 11.30 | < .001 | 96 | Left middle temporal gyrus | **PC × age** | -0.010 | 0.004 | -2.315 | **.021** |
| | 0.156 | 0.143 | 11.50 | < .001 | 154 | Left middle temporal gyrus | **PC × age** | -0.009 | 0.004 | -2.294 | **.022** |
| | 0.162 | 0.149 | 12.00 | < .001 | 157 | Left superior temporal gyrus | **PC** | 1.305 | 0.496 | 2.628 | **.009** |
| | 0.179 | 0.165 | 13.40 | < .001 | 232 | Right superior temporal gyrus | **PC** | 1.339 | 0.509 | 2.630 | **.009** |

Only significant PC-related terms are shown. Each row reports one significant term from the corresponding parcel-level GLM; consequently, the same parcel may appear more than once. Parcel indices refer to the Schaefer 400-parcel atlas. Adjusted $R^2$ = adjusted coefficient of determination; LANG = language network; PC = participation coefficient; SE = standard error.

## Discussion

The present study examined whether whole-brain rs-FC predicts individual differences in language performance in later adulthood, and how predictive information is distributed across a functionally defined language network and other large-scale systems. In addition, graph-theory analyses tested whether the topological organisation of the language network is associated with language ability, and whether age and education moderate these associations within a cohort of older adults. Together, the results converge on two conclusions: language-related predictive information is distributed across multiple functional systems, rather than confined to the language network, and the topological significance of the language network in predicting language performance is not uniform but depends on individual differences in education and age.

# Distributed network basis of language performance

CPM yielded significant out-of-sample predictions for both TPVT and READ scores from whole-brain rs-FC after adjusting for age, education, and head motion, consistent with prior evidence that resting-state connectivity encodes individual differences in language ability (Jiang et al., 2020; Tomasi & Volkow, 2020). The broader significance of this finding lies not in prediction accuracy per se, which was modest, in line with

prior connectome-based studies (Früh et al., 2025; Tomasi & Volkow, 2020), but in where predictive information was located: predominantly in connections between the language network and other large-scale systems, including the DMN, FPN, DAN, and VAN, rather than within the language network alone.

This pattern aligns with emerging accounts that reframe language not as a self-contained system but as a function depending on the coordinated activity of multiple large-scale networks (Forkel & Hagoort, 2024). Semantic cognition in particular has been characterised as requiring the interaction of at least two components, stored representations and executive control, subserved by partly distinct neural systems (Ralph et al., 2017). The DMN supports the representation and retrieval of semantic and conceptual knowledge, integrating distributed memory traces into coherent meaning (Binder et al., 2009; Fernandino & Binder, 2024); the FPN contributes goal-directed semantic control, modulating which aspects of meaning are activated and selected in context (Badre et al., 2005; Jefferies & Lambon Ralph, 2006); and the DAN and VAN may support attentional selection and reorienting during language processing (Corbetta & Shulman, 2002). That resting-state connectivity across all these systems carries predictive information about language ability in older adults extends this framework to an intrinsic, trait-level signal, suggesting that the functional architecture supporting language performance is not a specialised circuit but a property of how domain-general and language-specific networks are jointly organised at rest.

The two tasks engaged this distributed architecture in different ways, reflecting their distinct linguistic demands. TPVT requires listeners to map a spoken word onto its visual-conceptual referent, a process that engages auditory word form processing in bilateral superior temporal cortex, cross-modal semantic integration in anterior temporal regions, and access to rich lexico-conceptual knowledge distributed across the associative cortex (Binder et al., 2009; Davis & Johnsrude, 2003). This combination of auditory-linguistic, multimodal semantic, and controlled retrieval demands accounts well for the broad network signature observed. Vocabulary comprehension recruits not only core language regions but also the DMN-supported semantic store and FPN-mediated executive access to meaning, systems whose intrinsic connectivity organisation is reflected in resting-state FC. READ, by contrast, requires visual identification of familiar words and their pronunciation, engaging primarily the ventral occipito-temporal route for orthographic processing and the temporo-parietal route for grapheme-to-phoneme conversion (Dehaene & Cohen, 2011; Price, 2012). Its more constrained phonological and orthographic demands explain why predictive connectivity was more concentrated within the language network, with comparatively less involvement of broad associative systems. This task-differentiated pattern suggests that the degree to which whole-brain connectivity predicts language ability is sensitive to how extensively a given language task depends on cross-network integration beyond the core perisylvian system. The comparison with the Flanker task (see Appendix C), where sensorimotor edges were more prominent and largely absent from the language models, further supports the view that CPM edge profiles are broadly sensitive to processing demands, even when prediction is not task-exclusive.

The relatively modest predictive accuracy of the CPM models is itself informative. Resting-state FC reflects intrinsic functional organisation, which may not fully capture the task-engaged neural dynamics that vocabulary and reading assessments specifically recruit, a limitation consistent with evidence that task-based FC yields stronger language prediction than resting-state FC (Boyle et al., 2023; Jiang et al., 2020; Zhao et al., 2023). Beyond this, age and education are themselves strong determinants of language ability in older adults, and because they are partially encoded in brain connectivity patterns, adjusting for them statistically narrows the residual brain–behaviour signal available to the model (Früh et al., 2025; Krämer et al., 2023). Moreover, age-related changes in rs-FC involve complex, non-linear reorganisation that a linear adjustment cannot fully accommodate (Krämer et al., 2023), further limiting the variance in language performance that connectivity can explain independently of demographic factors in a later-adult sample. It bears emphasis that CPM identifies edges predictive of performance variability within a specific modelling context; the network composition of top-ranked edges is sensitive to sample characteristics, feature-selection thresholds, and regularisation choices, and should therefore be interpreted as descriptive and hypothesis-generating, rather than as evidence for independent network contributions to language performance.

## Language network topology and the moderating roles of education and age

The GLM analyses revealed that the relationship between language network topology and language performance was moderated by both education and age, with patterns that differed between the two tasks and between global efficiency and node-wise PC.

For vocabulary comprehension (TPVT), a significant interaction between language network global efficiency and education emerged. Among lower-educated individuals, better TPVT performance was associated with higher within-network efficiency, suggesting that efficient communication within the language network supports comprehension when formal linguistic experience is more limited, a pattern consistent with the cognitive reserve framework, in which individuals with lower reserve (for which education is a main proxy) may rely more on canonical neural resources to meet cognitive demands (Stern, 2009). Among higher-educated individuals, this relationship reversed: better TPVT performance was associated with lower within-network efficiency but higher PC across multiple left temporal, parietal, and frontal nodes, as well as right temporal regions. This pattern suggests that more highly educated individuals do not rely primarily on within-network connectivity, but instead benefit from a distributed topology of intermodular edges. In other words, the present results suggest that greater educational attainment is characterised by a more distributed neural signature of language processing, with greater between-networks coupling associated with more favorable language performance, consistent with evidence that education-related reserve involves stronger connectivity between key

hubs and task-relevant networks (Franzmeier et al., 2017). On the other hand, a more localized and segregated processing of language information seems to characterize individuals with lower education.

At the regional level, significant nodes spanned across cortical locations known to have a role in language processing, including: the left superior and middle temporal regions implicated in lexico-semantic processing (Binder et al., 2009), the left prefrontal cortex associated with controlled semantic retrieval (Badre & Wagner, 2007; Jackson, 2021; Whitney et al., 2011), and the right temporal regions involved in broader semantic and contextual integration beyond the core left-lateralised language system (Friederici, 2011); suggesting that cross-network hub function in these regions may be particularly sensitive to accumulated linguistic experience. The contrasting pattern observed for the Flanker task further suggests that the functional significance of language network topology is task-dependent: spatial overlap in significant nodes across tasks co-existed with systematic differences in directionality and moderation structure, indicating that cross-network integration in temporal and prefrontal cortex carries outcome-specific rather than generic functional meaning (Campbell & Tyler, 2018; Cole et al., 2013; Hagoort, 2013; Ralph et al., 2017).

Aside from the degree of educational attainment, age also moderated the PC–performance relationship for both tasks, with a consistent directional reversal across left temporal and left temporo-occipital regions. In relatively younger adults, higher PC in these nodes was associated with better performance, whereas in older adults the association reversed, such that lower PC was associated with better performance. The positive association between higher PC and performance in younger adults is consistent with the priorly reported evidence of a beneficial role of distributed connectivity in supporting language functions. Notably, this characteristic appears to be shared by participant groups with more favourable language-related profiles, namely younger and more highly educated individuals. Furthermore, temporal regions that emerged as significant have a known role in bridging the language network with the DMN and the FPN to support contextual inference and working memory during language processing (Rafiq et al., 2022; Zhang & Diaz, 2023). The opposite trend observed in older adults is compatible with, but does not establish, a neural dedifferentiation account: higher PC in this group may reflect a more distributed pattern of connectivity across network boundaries, which, when controlling for educational attainment, would be consistent with evidence linking dedifferentiation to poorer cognitive and language performance in aging (Chan et al., 2014; Deery et al., 2023; Geerligs et al., 2015). Broader conceptual frameworks such as the Scaffolding Theory of Aging and Cognition (STAC-r; Reuter-Lorenz & Park, 2014) suggest that the behavioural relevance of any connectivity feature is not static across the lifespan but shaped by cumulative biological and experiential factors; the present pattern is compatible with this view, though our data do not include direct measures of compensatory recruitment and cannot adjudicate between competing accounts.

## Task-specific topology effects

The node-wise PC analyses revealed partially overlapping but distinct anatomical profiles for TPVT and READ, likely reflecting their different processing demands. For TPVT, significant PC effects spanned a broader frontotemporal network across seven parcels, and education moderation predominated, consistent with the distributed lexico-semantic and comprehension demands of the task and the sensitivity of accumulated linguistic experience to those demands (Binder et al., 2009; Tomasi & Volkow, 2020). For READ, significant effects were concentrated in four parcels, and no significant education interactions, consistent with the more constrained phonological and orthographic demands of single-word reading and the established role of ventral occipito-temporal cortex in orthographic processing and grapheme-to-phoneme conversion (Dehaene & Cohen, 2011).

The left posterior superior temporal sulcus was the only region with significant PC effects for both tasks, but in opposite directions: negative for TPVT and positive for READ. This region sits at the intersection of dorsal phonological and ventral semantic processing streams (Binder et al., 2009; Friederici, 2011). For READ, a more connector-like profile at this node even in condition of resting state may support coordination of orthographic, phonological, and semantic information, whereas for TPVT, which relies on spoken-word comprehension and lexico-semantic access without orthographic demands, a more focal connectivity profile may be advantageous, consistent with flexible network accounts of language processing (Liebenthal et al., 2014; Wilson et al., 2018). This dissociation merits direct examination in future work combining task-based and resting-state fMRI.

## Limitations

Some limitations should be considered when interpreting the present findings. First, the use of rs-FC as the sole neural predictor places an inherent ceiling on predictive performance. Resting-state FC reflects intrinsic functional organisation but does not directly capture the task-evoked processes engaged during language assessment, including moment-to-moment strategy, memory retrieval, and task-specific demands. This gap between intrinsic and task-engaged states likely contributes to the modest predictive performance observed, and is compounded by the greater variability and weaker connectivity signal characteristic of resting-state data in older adults relative to younger populations.

Second, the behavioural scope is limited to two specific components of language ability. TPVT and READ capture lexical-semantic knowledge and single-word reading decoding, both largely crystallised abilities shaped by accumulated educational and cultural experience (Gershon et al., 2014). More dynamic aspects of language, such as sentence comprehension, syntactic processing, and pragmatic inference, involve greater

online integration of linguistic information and may have distinct neural substrates. The present findings are therefore most directly informative about vocabulary knowledge and word recognition and should not be generalised to the broader language domain.

Third, the language network definition was necessarily atlas- and method-dependent. Nodes were identified by overlapping a group-level resting-state language map (Branco et al., 2020) with the Schaefer 400-parcel atlas (Schaefer et al., 2018), using a 51% volumetric overlap criterion. While this procedure is transparent and reproducible, alternative atlas resolutions, probabilistic thresholds, or overlap criteria could yield a different set of language parcels and influence the pattern of results accordingly.

Finally, several analytical choices, including the consensus edge stability criterion in CPM, the FDR-based graph thresholding, and the selection of graph-theoretical metrics, followed established approaches in the literature to facilitate comparability and interpretation. These choices are not uniquely optimal, however, and alternative implementations may yield somewhat different findings. Meanwhile, CPM performance remains to be validated in an independent sample. The composition of the top-ranked edge sets may be sample- and analysis-dependent; accordingly, raw network counts should be interpreted descriptively rather than as formal evidence of network enrichment.

Future work employing complementary methodological approaches will be important for establishing the robustness of the present results.

## Conclusions

The present study demonstrates that individual differences in language performance in later adulthood are predicted by distributed inter-network functional connectivity. This positions language performance in ageing as a whole-brain phenomenon, underpinned by domain-general systems that also support semantic memory, controlled retrieval, and executive function. Complementing this, the topological organisation of the language network was associated with language performance in ways that were systematically moderated by education and age, tentatively suggesting a shift from more localized to distributed processing with increasing linguistic experience (tied to greater education attainment) and younger age. Together, these findings call for a shift away from language network-centric models towards frameworks that foreground whole-brain network dynamics and their interaction with life-course factors. Future work in larger and more diverse samples, combining resting-state and task-based fMRI, will be needed to establish the generalisability of these findings. Ultimately, a richer understanding of the distributed network basis of language in healthy ageing may have downstream implications for clinical practice: if language ability depends on the integrity of broadly distributed systems rather than solely on focal language regions, this perspective could inform the diagnosis and prognosis of language disorders such as post-stroke aphasia and primary progressive aphasia, where residual network capacity may help recovery trajectories, and could also inform the design of rehabilitation approaches that target domain-general network support alongside language-specific processing.

## Declarations

# Conflict of interest

The Authors disclose no conflict of interest.

# Author contribution statement

I.B. and X.L. contributed to conceptualization, methodology, and writing of the original draft; I.B. additionally conducted the formal analyses and prepared all figures. A.M. and A.V. contributed to conceptualization, supervised the project, and critically reviewed and edited the manuscript. All authors read and approved the final version.

# Fundings

The authors declare that no funds, grants, or other support were received during the preparation of this manuscript.

# Author Contribution

I.B. and X.L. contributed to conceptualization, methodology, and writing of the original draft; I.B. additionally conducted the formal analyses and prepared all figures. A.M. and A.V. contributed to conceptualization, supervised the project, and critically reviewed and edited the manuscript. All authors read and approved the final version.

## Acknowledgement

Data and/or research tools used in the preparation of this manuscript were obtained from the National Institute of Mental Health (NIMH) Data Archive (NDA). NDA is a collaborative informatics system created by the National Institutes of Health to provide a national resource to support and accelerate research in mental health. Dataset identifier(s): 10.15154/rw5y-ge69. This manuscript reflects the views of the authors and may not reflect the opinions or views of the NIH or of the Submitters submitting original data to NDA.

## Data Availability

The resting-state fMRI and behavioural data analysed in this study are not publicly available in their raw form but are accessible to approved researchers through the Human Connectome Project Lifespan Aging dataset (HCP-A; https://www.humanconnectome.org/study/hcp-lifespan-aging). Access requires registration and agreement with the HCP data use terms. Analyses' codes are available in GitHub (https://github.com/irenebellin/CPM_graph_language).

## References

1. Badre D, Poldrack RA, Paré-Blagoev EJ, Insler RZ, Wagner AD (2005) Dissociable Controlled Retrieval and Generalized Selection Mechanisms in Ventrolateral Prefrontal Cortex. Neuron 47(6):907–918. https://doi.org/10.1016/j.neuron.2005.07.023
2. Badre D, Wagner AD (2007) Left ventrolateral prefrontal cortex and the cognitive control of memory. Neuropsychologia 45(13):2883–2901. https://doi.org/10.1016/j.neuropsychologia.2007.06.015
3. Binder JR, Desai RH, Graves WW, Conant LL (2009) Where Is the Semantic System? A Critical Review and Meta-Analysis of 120 Functional Neuroimaging Studies. Cereb Cortex 19(12):2767–2796. https://doi.org/10.1093/cercor/bhp055
4. Boyle R, Connaughton M, McGlinchey E, Knight SP, De Looze C, Carey D, Stern Y, Robertson IH, Kenny RA, Whelan R (2023) Connectome-based predictive modelling of cognitive reserve using task-based functional connectivity. Eur J Neurosci 57(3):490–510. https://doi.org/10.1111/ejn.15896
5. Bozzano A, Barletta L, Caneva S, Truffelli M, Bennicelli E, Rebella G, Zona G, Castellan L (2025) Resting-State fMRI to Map Language Function for Surgical Planning in Patients With Brain Tumors: A Feasibility Study. J Neuroimaging 35(1):e70027. https://doi.org/10.1111/jon.70027
6. Braga RM, Buckner RL (2017) Parallel Interdigitated Distributed Networks within the Individual Estimated by Intrinsic Functional Connectivity. Neuron 95(2):457–471e5. https://doi.org/10.1016/j.neuron.2017.06.038
7. Braga RM, DiNicola LM, Becker HC, Buckner RL (2020) Situating the left-lateralized language network in the broader organization of multiple specialized large-scale distributed networks. J Neurophysiol 124(5):1415–1448. https://doi.org/10.1152/jn.00753.2019
8. Branco P, Seixas D, Castro SL (2020) Mapping language with resting-state functional magnetic resonance imaging: A study on the functional profile of the language network. Hum Brain Mapp 41(2):545–560. https://doi.org/10.1002/hbm.24821
9. Broca P (1865) *Localization of speech in the third left frontal convolution.*
10. Campbell KL, Tyler LK (2018) Language-related domain-specific and domain-general systems in the human brain. Curr Opin Behav Sci 21:132–137. https://doi.org/10.1016/j.cobeha.2018.04.008
11. Chai LR, Mattar MG, Blank IA, Fedorenko E, Bassett DS (2016) Functional Network Dynamics of the Language System. Cereb Cortex 26(11):4148–4159. https://doi.org/10.1093/cercor/bhw238
12. Chan MY, Park DC, Savalia NK, Petersen SE, Wig GS (2014) Decreased segregation of brain systems across the healthy adult lifespan. *Proceedings of the National Academy of Sciences*, *111*(46). https://doi.org/10.1073/pnas.1415122111
13. Cole MW, Ito T, Bassett DS, Schultz DH (2016) Activity flow over resting-state networks shapes cognitive task activations. Nat Neurosci 19(12):1718–1726. https://doi.org/10.1038/nn.4406
14. Cole MW, Reynolds JR, Power JD, Repovs G, Anticevic A, Braver TS (2013) Multi-task connectivity reveals flexible hubs for adaptive task control. Nat Neurosci 16(9):1348–1355. https://doi.org/10.1038/nn.3470
15. Corbetta M, Shulman GL (2002) Control of goal-directed and stimulus-driven attention in the brain. Nat Rev Neurosci 3(3):201–215. https://doi.org/10.1038/nrn755
16. Davis MH, Johnsrude IS (2003) Hierarchical Processing in Spoken Language Comprehension. J Neurosci 23(8):3423–3431. https://doi.org/10.1523/JNEUROSCI.23-08-03423.2003
17. Deery HA, Di Paolo R, Moran C, Egan GF, Jamadar SD (2023) The older adult brain is less modular, more integrated, and less efficient at rest: A systematic review of large-scale resting-state functional brain networks in aging. Psychophysiology 60(1):e14159. https://doi.org/10.1111/psyp.14159

18. Dehaene S, Cohen L (2011) The unique role of the visual word form area in reading. Trends Cogn Sci 15(6):254–262. https://doi.org/10.1016/j.tics.2011.04.003
19. Dronkers NF, Wilkins DP, Van Valin RD, Redfern BB, Jaeger JJ (2004) Lesion analysis of the brain areas involved in language comprehension. Cognition 92(1–2):145–177. https://doi.org/10.1016/j.cognition.2003.11.002
20. Elam JS, Glasser MF, Harms MP, Sotiropoulos SN, Andersson JLR, Burgess GC, Curtiss SW, Oostenveld R, Larson-Prior LJ, Schoffelen J-M, Hodge MR, Cler EA, Marcus DM, Barch DM, Yacoub E, Smith SM, Ugurbil K, Van Essen DC (2021) The Human Connectome Project: A retrospective. NeuroImage 244:118543. https://doi.org/10.1016/j.neuroimage.2021.118543
21. Fedorenko E, Hsieh P-J, Nieto-Castañón A, Whitfield-Gabrieli S, Kanwisher N (2010) New Method for fMRI Investigations of Language: Defining ROIs Functionally in Individual Subjects. J Neurophysiol 104(2):1177–1194. https://doi.org/10.1152/jn.00032.2010
22. Fedorenko E, Ivanova AA, Regev TI (2024) The language network as a natural kind within the broader landscape of the human brain. Nat Rev Neurosci 25(5):289–312. https://doi.org/10.1038/s41583-024-00802-4
23. Fernandino L, Binder JR (2024) How does the default mode network contribute to semantic cognition? Brain Lang 252:105405. https://doi.org/10.1016/j.bandl.2024.105405
24. Forkel SJ, Hagoort P (2024) Redefining language networks: Connectivity beyond localised regions. Brain Struct Function 229(9):2073–2078. https://doi.org/10.1007/s00429-024-02859-4
25. Franzmeier N, Göttler J, Grimmer T, Drzezga A, Áraque-Caballero MA, Simon-Vermot L, Taylor ANW, Bürger K, Catak C, Janowitz D, Müller C, Duering M, Sorg C, Ewers M (2017) Resting-State Connectivity of the Left Frontal Cortex to the Default Mode and Dorsal Attention Network Supports Reserve in Mild Cognitive Impairment. Front Aging Neurosci 9:264. https://doi.org/10.3389/fnagi.2017.00264
26. Friederici AD (2011) The Brain Basis of Language Processing: From Structure to Function. Physiol Rev 91(4):1357–1392. https://doi.org/10.1152/physrev.00006.2011
27. Früh D, Mendl-Heinisch C, Bittner N, Weis S, Caspers S (2025) Prediction of Verbal Abilities From Brain Connectivity Data Across the Lifespan Using a Machine Learning Approach. Hum Brain Mapp 46(5):e70191. https://doi.org/10.1002/hbm.70191
28. Geerligs L, Renken RJ, Saliasi E, Maurits NM, Lorist MM (2015) A Brain-Wide Study of Age-Related Changes in Functional Connectivity. Cereb Cortex 25(7):1987–1999. https://doi.org/10.1093/cercor/bhu012
29. Gershon RC, Cook KF, Mungas D, Manly JJ, Slotkin J, Beaumont JL, Weintraub S (2014) Language Measures of the NIH Toolbox Cognition Battery. J Int Neuropsychol Soc 20(6):642–651. https://doi.org/10.1017/S1355617714000411
30. Geschwind N (1965) DISCONNEXION SYNDROMES IN ANIMALS AND MAN. Brain 88(2):237–237. https://doi.org/10.1093/brain/88.2.237
31. Glasser MF, Smith SM, Marcus DS, Andersson JLR, Auerbach EJ, Behrens TEJ, Coalson TS, Harms MP, Jenkinson M, Moeller S, Robinson EC, Sotiropoulos SN, Xu J, Yacoub E, Ugurbil K, Van Essen DC (2016) The Human Connectome Project's neuroimaging approach. Nat Neurosci 19(9):1175–1187. https://doi.org/10.1038/nn.4361
32. Glasser MF, Sotiropoulos SN, Wilson JA, Coalson TS, Fischl B, Andersson JL, Xu J, Jbabdi S, Webster M, Polimeni JR, Van Essen DC, Jenkinson M (2013) The minimal preprocessing pipelines for the Human Connectome Project. NeuroImage 80:105–124. https://doi.org/10.1016/j.neuroimage.2013.04.127
33. Gratton C, Laumann TO, Nielsen AN, Greene DJ, Gordon EM, Gilmore AW, Nelson SM, Coalson RS, Snyder AZ, Schlaggar BL, Dosenbach NUF, Petersen SE (2018) Functional Brain Networks Are Dominated by Stable Group and Individual Factors, Not Cognitive or Daily Variation. Neuron 98(2):439–452e5. https://doi.org/10.1016/j.neuron.2018.03.035
34. Guichet C, Banjac S, Achard S, Mermillod M, Baciu M (2024) Modeling the neurocognitive dynamics of language across the lifespan. Hum Brain Mapp 45(5):e26650. https://doi.org/10.1002/hbm.26650
35. Hagoort P (2013) MUC (Memory, Unification, Control) and beyond. Front Psychol. *4*https://doi.org/10.3389/fpsyg.2013.00416
36. Harms MP, Somerville LH, Ances BM, Andersson J, Barch DM, Bastiani M, Bookheimer SY, Brown TB, Buckner RL, Burgess GC, Coalson TS, Chappell MA, Dapretto M, Douaud G, Fischl B, Glasser MF, Greve DN, Hodge C, Jamison KW, Yacoub E (2018) Extending the Human Connectome Project across ages: Imaging protocols for the Lifespan Development and Aging projects. NeuroImage 183:972–984. https://doi.org/10.1016/j.neuroimage.2018.09.060
37. Jackson RL (2021) The neural correlates of semantic control revisited. NeuroImage 224:117444. https://doi.org/10.1016/j.neuroimage.2020.117444
38. Jefferies E, Lambon Ralph MA (2006) Semantic impairment in stroke aphasia versus semantic dementia: A case-series comparison. Brain 129(8):2132–2147. https://doi.org/10.1093/brain/awl153
39. Jiang R, Zuo N, Ford JM, Qi S, Zhi D, Zhuo C, Xu Y, Fu Z, Bustillo J, Turner JA, Calhoun VD, Sui J (2020) Task-induced brain connectivity promotes the detection of individual differences in brain-behavior relationships. NeuroImage 207:116370. https://doi.org/10.1016/j.neuroimage.2019.116370
40. Krämer C, Stumme J, Campos DC, Rubbert L, Caspers C, Caspers J, S., Jockwitz C (2023) Classification and prediction of cognitive performance differences in older age based on brain network patterns using a machine learning approach. Netw Neurosci 7(1):122–147.

https://doi.org/10.1162/netn_a_00275

41. Liebenthal E, Desai RH, Humphries C, Sabri M, Desai A (2014) The functional organization of the left STS: A large scale meta-analysis of PET and fMRI studies of healthy adults. *Frontiers in Neuroscience*, *8*. https://doi.org/10.3389/fnins.2014.00289
42. Lipkin B, Tuckute G, Affourtit J, Small H, Mineroff Z, Kean H, Jouravlev O, Rakocevic L, Pritchett B, Siegelman M, Hoeflin C, Pongos A, Blank IA, Struhl MK, Ivanova A, Shannon S, Sathe A, Hoffmann M, Nieto-Castañón A, Fedorenko E (2022) Probabilistic atlas for the language network based on precision fMRI data from > 800 individuals. Sci Data 9(1):529. https://doi.org/10.1038/s41597-022-01645-3
43. Malik-Moraleda S, Ayyash D, Gallée J, Affourtit J, Hoffmann M, Mineroff Z, Jouravlev O, Fedorenko E (2022) An investigation across 45 languages and 12 language families reveals a universal language network. Nat Neurosci 25(8):1014–1019. https://doi.org/10.1038/s41593-022-01114-5
44. Marcus DS, Harms MP, Snyder AZ, Jenkinson M, Wilson JA, Glasser MF, Barch DM, Archie KA, Burgess GC, Ramaratnam M, Hodge M, Horton W, Herrick R, Olsen T, McKay M, House M, Hileman M, Reid E, Harwell J, Van Essen DC (2013) Human Connectome Project informatics: Quality control, database services, and data visualization. NeuroImage 80:202–219. https://doi.org/10.1016/j.neuroimage.2013.05.077
45. Menardi A, Spoa M, Vallesi A (2024) Brain topology underlying executive functions across the lifespan: Focus on the default mode network. Front Psychol 15:1441584. https://doi.org/10.3389/fpsyg.2024.1441584
46. Morishima Y, Van Den Heuvel M, Strik W, Dierks T (2025) Neurobiologically informed graph theory analysis of the language system. Netw Neurosci 9(2):504–521. https://doi.org/10.1162/netn_a_00443
47. Park KY, Lee JJ, Dierker D, Marple LM, Hacker CD, Roland JL, Marcus DS, Milchenko M, Miller-Thomas MM, Benzinger TL, Shimony JS, Snyder AZ, Leuthardt EC (2020) Mapping language function with task-based vs. Resting-state functional MRI. PLoS ONE 15(7):e0236423. https://doi.org/10.1371/journal.pone.0236423
48. Price CJ (2012) A review and synthesis of the first 20 years of PET and fMRI studies of heard speech, spoken language and reading. NeuroImage 20 YEARS fMRI 62(2):816–847. https://doi.org/10.1016/j.neuroimage.2012.04.062
49. Rafiq M, Jucla M, Guerrier L, Péran P, Pariente J, Pistono A (2022) The functional connectivity of language network across the life span: Disentangling the effects of typical aging from Alzheimer's disease. Front Aging Neurosci 14:959405. https://doi.org/10.3389/fnagi.2022.959405
50. Ralph MAL, Jefferies E, Patterson K, Rogers TT (2017) The neural and computational bases of semantic cognition. Nat Rev Neurosci 18(1):42–55. https://doi.org/10.1038/nrn.2016.150
51. Reuter-Lorenz PA, Park DC (2014) How Does it STAC Up? Revisiting the Scaffolding Theory of Aging and Cognition. Neuropsychol Rev 24(3):355–370. https://doi.org/10.1007/s11065-014-9270-9
52. Rubinov M, Sporns O (2010) Complex network measures of brain connectivity: Uses and interpretations. NeuroImage 52(3):1059–1069. https://doi.org/10.1016/j.neuroimage.2009.10.003
53. Schaefer A, Kong R, Gordon EM, Laumann TO, Zuo X-N, Holmes AJ, Eickhoff SB, Yeo BTT (2018) Local-Global Parcellation of the Human Cerebral Cortex from Intrinsic Functional Connectivity MRI. Cereb Cortex 28(9):3095–3114. https://doi.org/10.1093/cercor/bhx179
54. Shen X, Finn ES, Scheinost D, Rosenberg MD, Chun MM, Papademetris X, Constable RT (2017) Using connectome-based predictive modeling to predict individual behavior from brain connectivity. Nat Protoc 12(3):506–518. https://doi.org/10.1038/nprot.2016.178
55. Smith SM, Fox PT, Miller KL, Glahn DC, Fox PM, Mackay CE, Filippini N, Watkins KE, Toro R, Laird AR, Beckmann CF (2009) Correspondence of the brain's functional architecture during activation and rest. *Proceedings of the National Academy of Sciences*, *106*(31), 13040–13045. https://doi.org/10.1073/pnas.0905267106
56. Stern Y (2009) Cognitive reserve. Neuropsychologia 47(10):2015–2028. https://doi.org/10.1016/j.neuropsychologia.2009.03.004
57. Stumme J, Jockwitz C, Hoffstaedter F, Amunts K, Caspers S (2020) Functional network reorganization in older adults: Graph-theoretical analyses of age, cognition and sex. NeuroImage 214:116756. https://doi.org/10.1016/j.neuroimage.2020.116756
58. De Thiebaut M, Foulon C, Nachev P (2020) Brain disconnections link structural connectivity with function and behaviour. Nat Commun 11(1):5094. https://doi.org/10.1038/s41467-020-18920-9
59. Thomas Yeo BT, Krienen FM, Sepulcre J, Sabuncu MR, Lashkari D, Hollinshead M, Roffman JL, Smoller JW, Zöllei L, Polimeni JR, Fischl B, Liu H, Buckner RL (2011) The organization of the human cerebral cortex estimated by intrinsic functional connectivity. J Neurophysiol 106(3):1125–1165. https://doi.org/10.1152/jn.00338.2011
60. Tomasi D, Volkow ND (2020) Network connectivity predicts language processing in healthy adults. Hum Brain Mapp 41(13):3696–3708. https://doi.org/10.1002/hbm.25042
61. Vigneau M, Beaucousin V, Hervé PY, Duffau H, Crivello F, Houdé O, Mazoyer B, Tzourio-Mazoyer N (2006) Meta-analyzing left hemisphere language areas: Phonology, semantics, and sentence processing. NeuroImage 30(4):1414–1432. https://doi.org/10.1016/j.neuroimage.2005.11.002

62. Vogel AC, Church JA, Power JD, Miezin FM, Petersen SE, Schlaggar BL (2013) Functional network architecture of reading-related regions across development. Brain Lang 125(2):231–243. https://doi.org/10.1016/j.bandl.2012.12.016
63. Wernicke C (1874) Der aphasische Symptomencomplex: Eine psychologische Studie auf anatomischer Basis. Max Cohn&Weigert.), Breslau
64. Whitney C, Kirk M, O'Sullivan J, Lambon Ralph MA, Jefferies E (2011) The Neural Organization of Semantic Control: TMS Evidence for a Distributed Network in Left Inferior Frontal and Posterior Middle Temporal Gyrus. Cereb Cortex 21(5):1066–1075. https://doi.org/10.1093/cercor/bhq180
65. Wilson SM, Bautista A, McCarron A (2018) Convergence of spoken and written language processing in the superior temporal sulcus. NeuroImage 171:62–74. https://doi.org/10.1016/j.neuroimage.2017.12.068
66. Zhang H, Diaz MT (2023) Resting State Network Segregation Modulates Age-Related Differences in Language Production. Neurobiol Lang 4(2):382–403. https://doi.org/10.1162/nol_a_00106
67. Zhao W, Makowski C, Hagler DJ, Garavan HP, Thompson WK, Greene DJ, Jernigan TL, Dale AM (2023) Task fMRI paradigms may capture more behaviorally relevant information than resting-state functional connectivity. NeuroImage 270:119946. https://doi.org/10.1016/j.neuroimage.2023.119946

## Figures

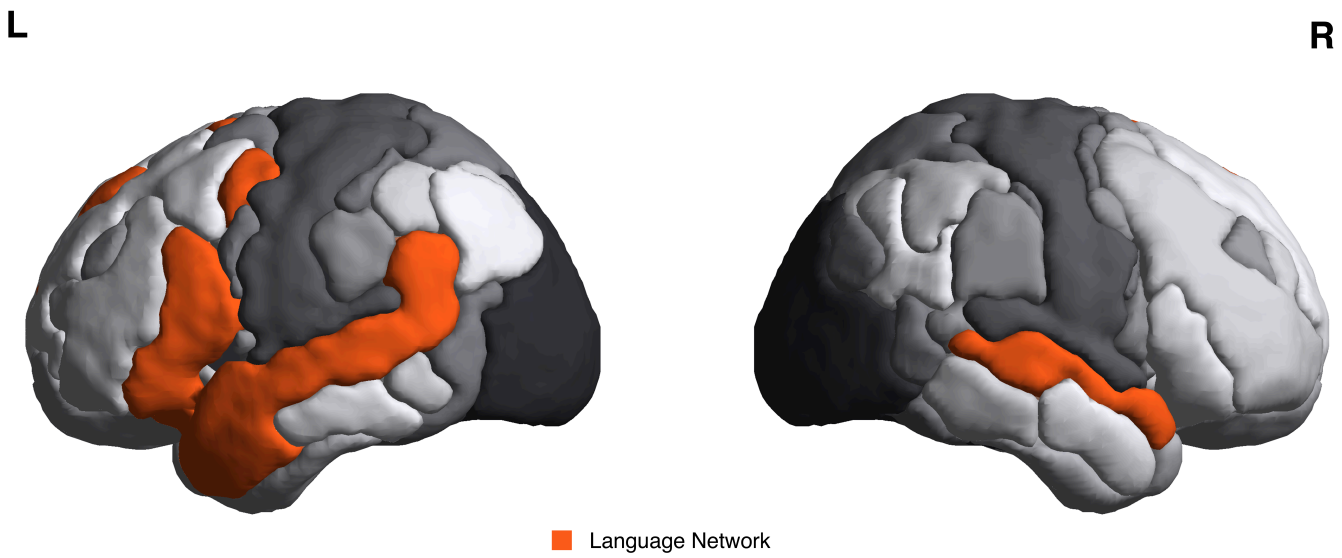



**Figure 1**

**Sagittal view of the Schaefer 400-parcel atlas re-parcellated into eight functional networks.** The language network is highlighted in orange, while the seven canonical resting-state networks are depicted in varying shades of grey.

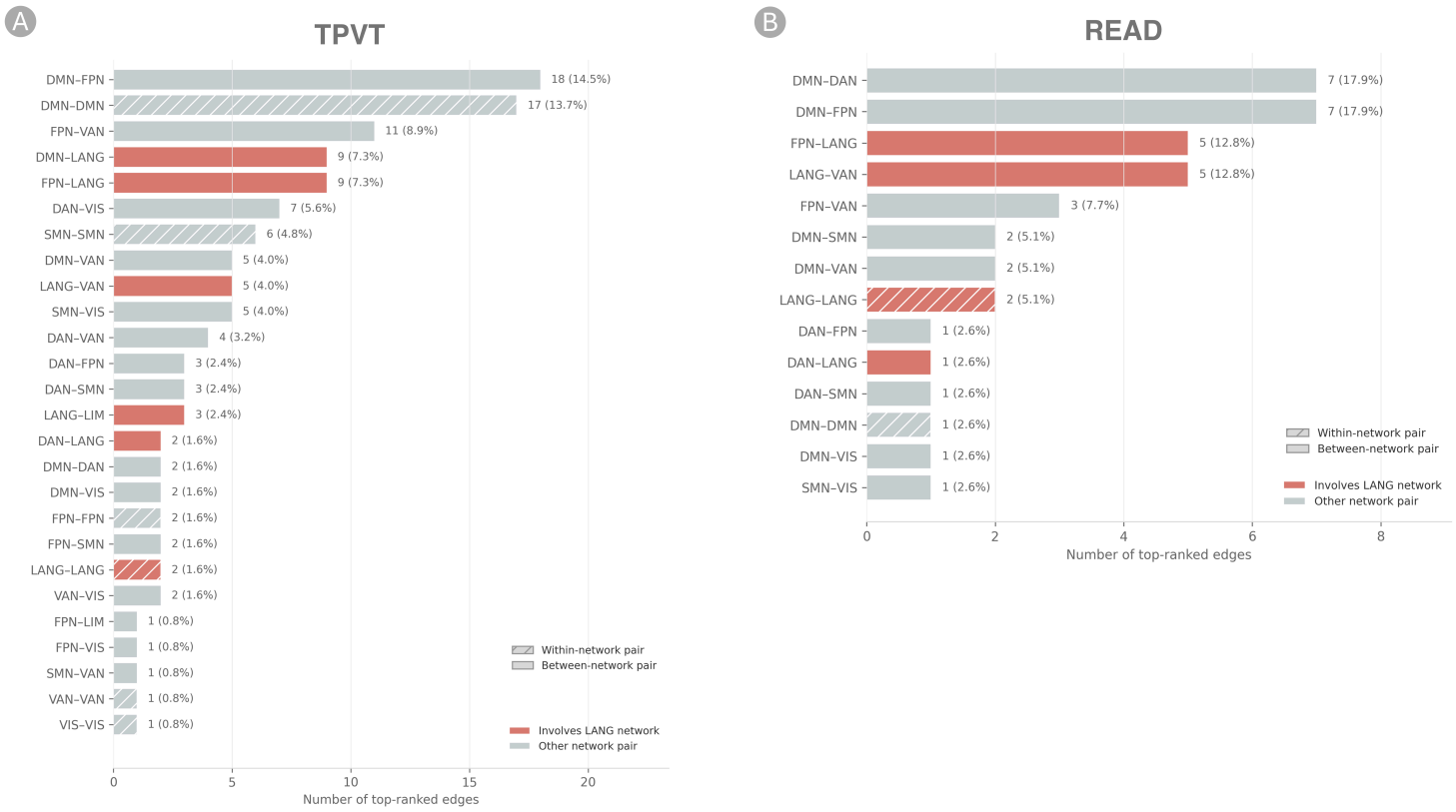



**Figure 2**

**Network-pair representation among top-ranked edges in the primary CPM models for TPVT (Panel A; n = 124 edges) and READ (Panel B; n = 39 edges).** Bars represent the number of top-ranked edges assigned to each network pair in the primary fully adjusted CPM models. Percentages are relative to the total number of top-ranked edges within each model.

DAN = dorsal attention network; DMN = default mode network; FPN = frontoparietal network; LANG = language network; LIM = limbic network; SMN = somatomotor network; VAN = ventral attention network; VIS = visual network.




**Figure 3**

**Composition and anatomical distribution of top-ranked edges in the primary CPM models for TPVT and READ.** Panel A shows the intra- and inter-network breakdown of top-ranked edges. Panel B shows the endpoint-network representation, with bars indicating the number of edge endpoints belonging to each network; percentages are relative to the total number of endpoints within each behavioural measure. Panels C and D show the anatomical distribution of top-ranked edges for TPVT (n = 124) and READ (n = 39), respectively; grey circles represent Schaefer 400 cortical parcels, coloured lines represent top-ranked edges, and edge colour encodes the signed model-based predictive contribution, with warmer and cooler colours indicating positive and negative contributions. Anatomical left is displayed on the left, right is on the right. DAN = dorsal attention network; DMN = default mode network; FPN = frontoparietal network; LANG = language network; LIM = limbic network; SMN = somatomotor network; VAN = ventral attention network; VIS = visual network.

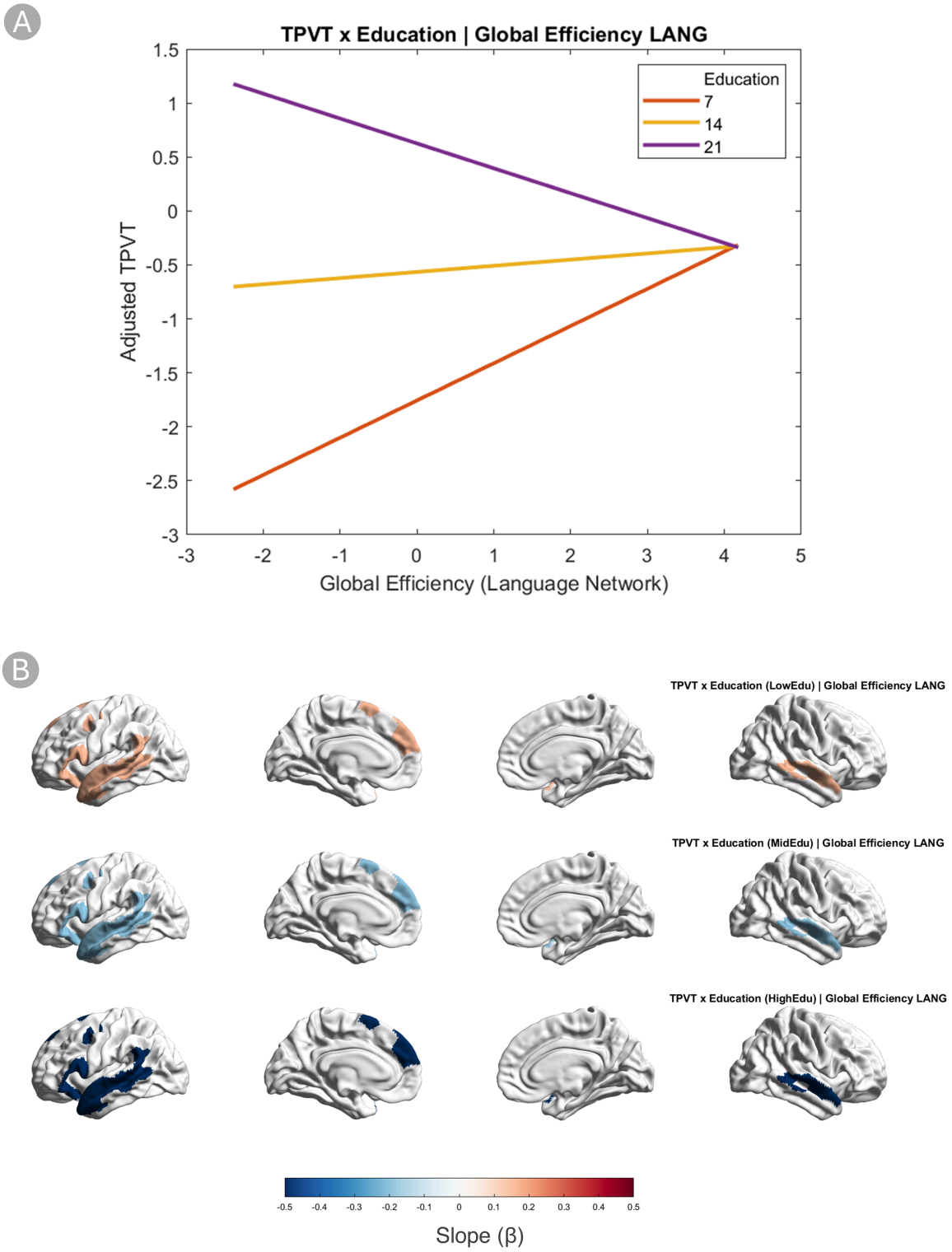



**Figure 4**

**Interaction between education and LANG global efficiency for TPVT**. Panel (a) shows model-estimated associations between LANG global efficiency and TPVT performance at representative levels of 7, 14, and 21 years of education. Panel (b) displays the LANG mask at these education levels, coloured uniformly according to the corresponding conditional coefficients for global efficiency. LANG = language network.

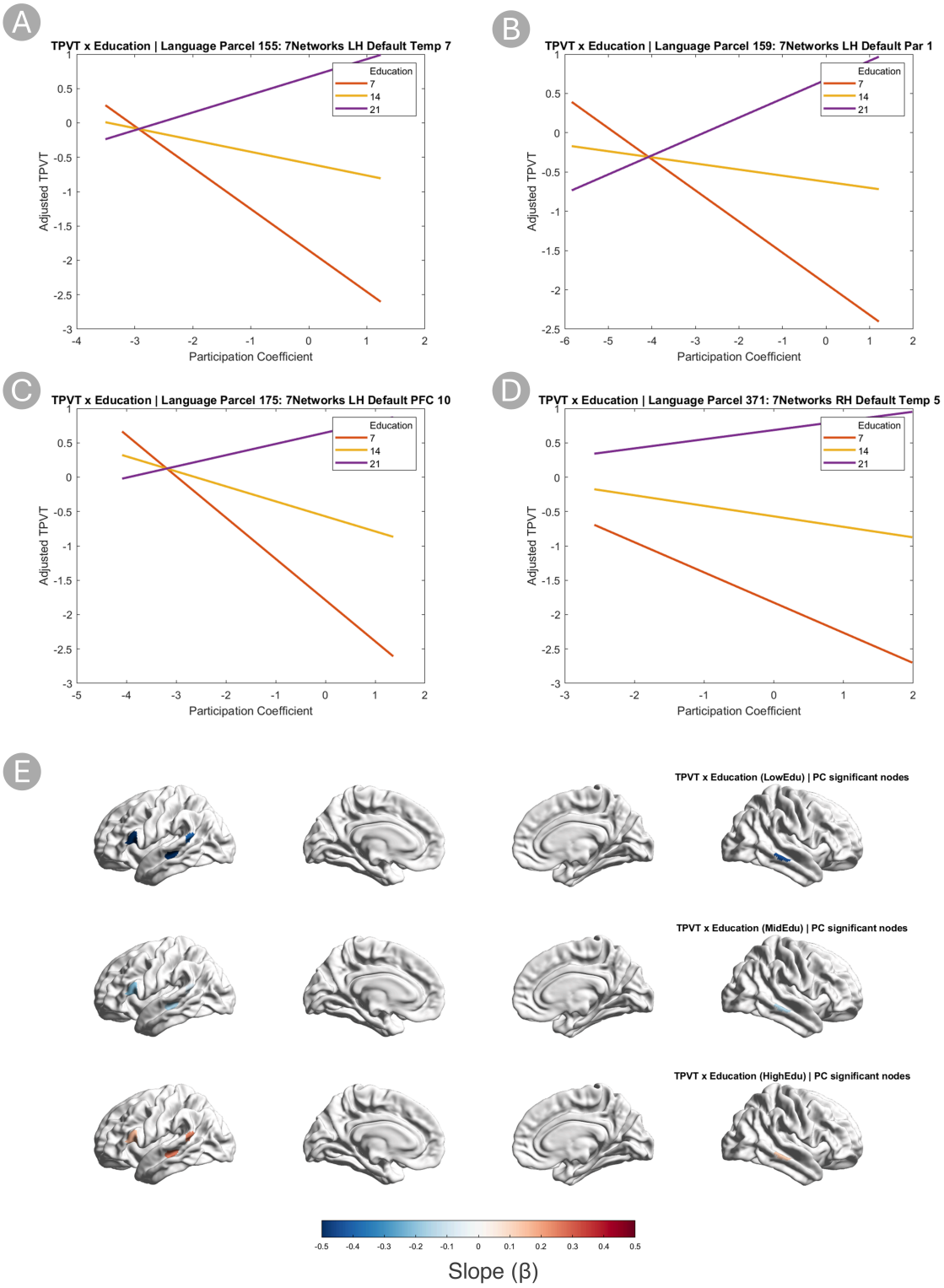



**Figure 5**

**Education interactions between node-wise PC and TPVT performance**. Panels (a)–(d) show model-estimated associations between PC and TPVT performance at 7, 14, and 21 years of education for parcels with significant PC × education interactions. Panel (e) maps the corresponding parcel-specific conditional PC coefficients at the same education levels. PC = participation coefficient.

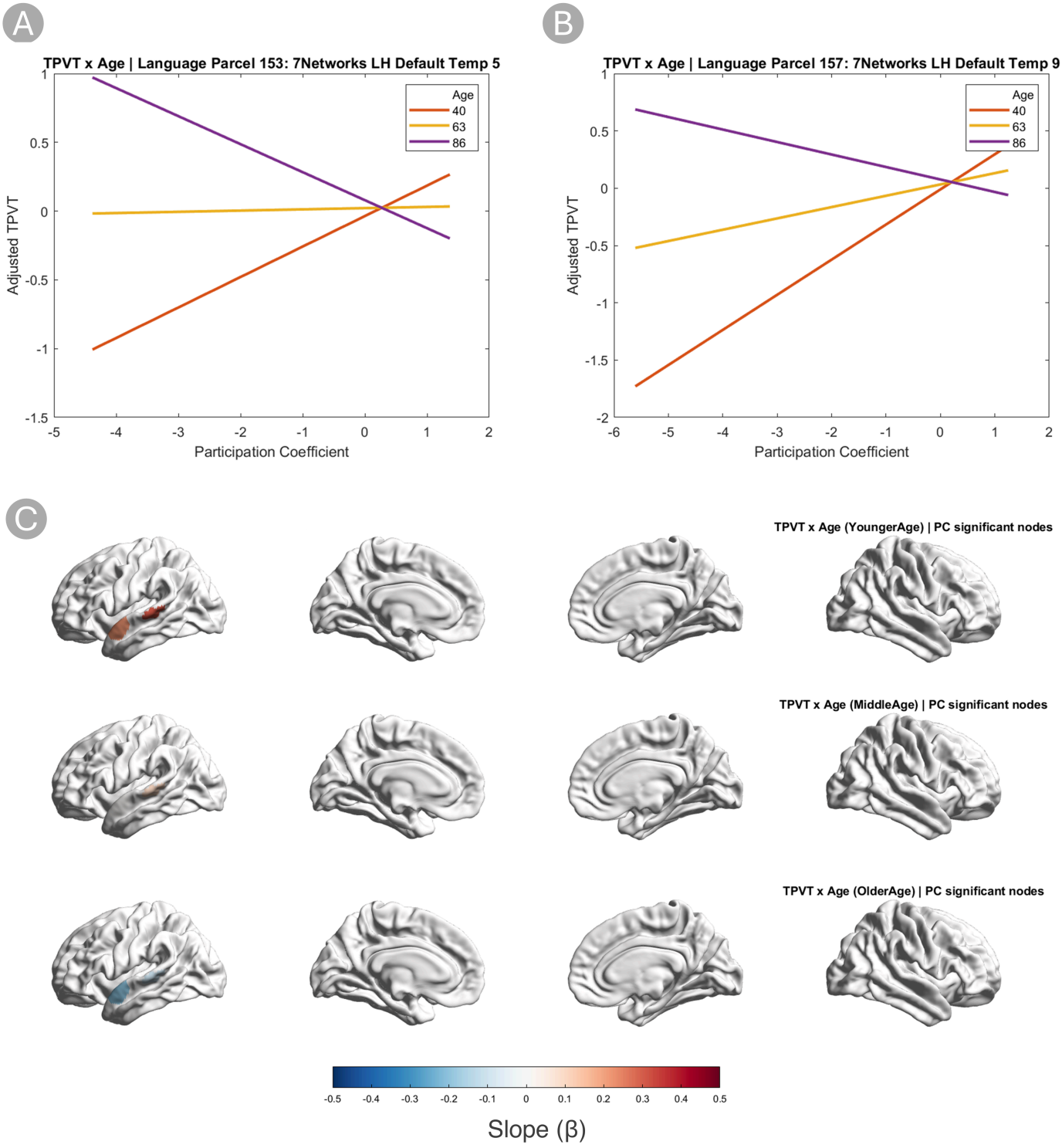



**Figure 6**

**Age interactions between node-wise PC and TPVT performance**. Panels (a)–(b) show model-estimated associations between PC and TPVT performance at 40, 63, and 86 years of age for parcels with significant PC × age interactions. Panel (c) maps the corresponding parcel-specific conditional PC coefficients at the same age levels. PC = participation coefficient.

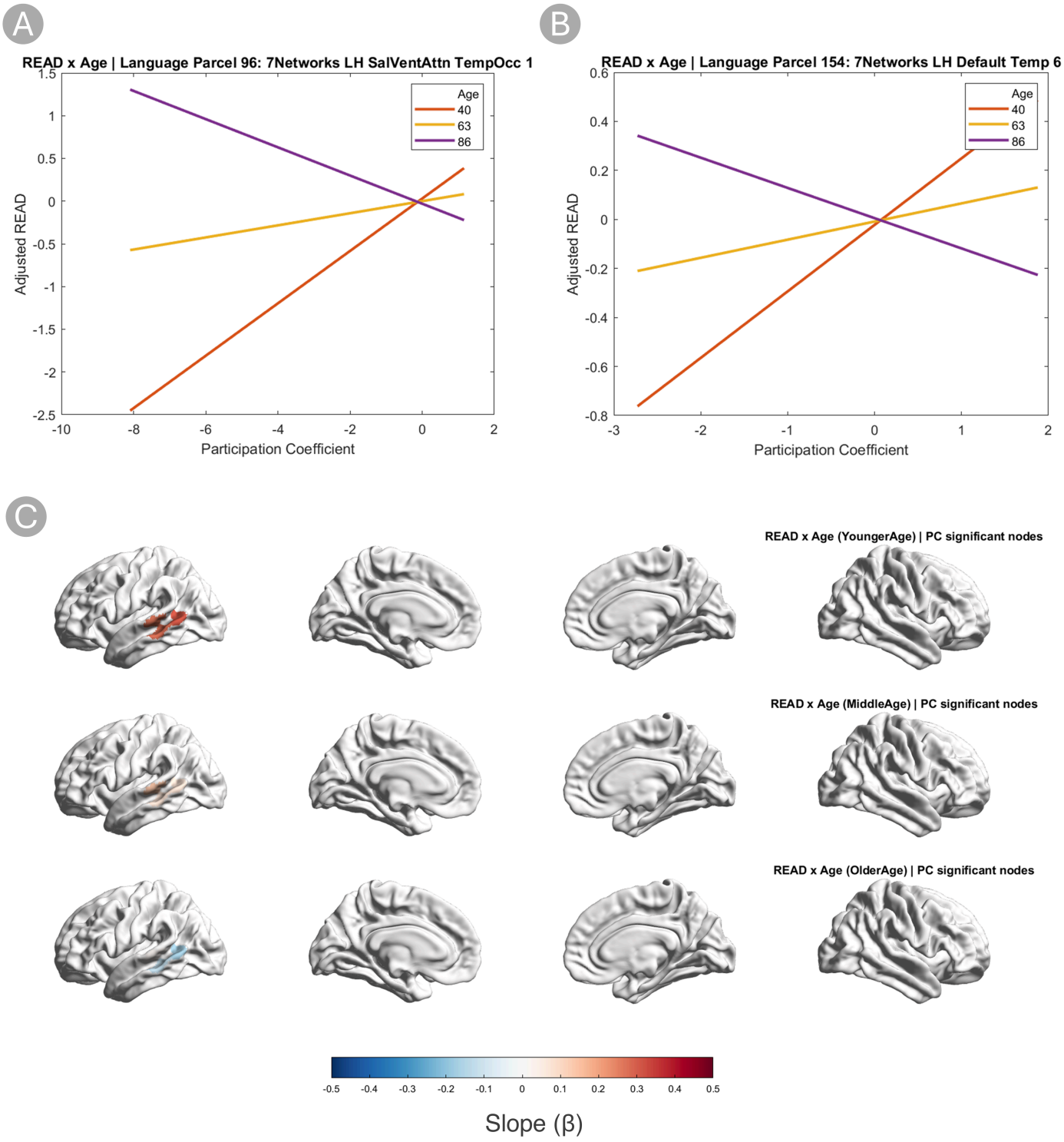



**Figure 7**

**Age interactions between node-wise PC and READ performance**. Panels (a)–(b) show model-estimated associations between PC and READ performance at 40, 63, and 86 years of age for parcels with significant PC × age interactions. Panel (c) maps the corresponding parcel-specific conditional PC coefficients at the same age levels. PC = participation coefficient.

## Supplementary Files

This is a list of supplementary files associated with this preprint. Click to download.

- SupplementaryMaterials.pdf